Giant Al-M (M = transitional metal) crystals as Penrose-tiling approximants of the decagonal quasicrystal

H. Zhang
Beijing Laboratory of Electron Microscopy, Chinese Academy of Sciences, P.O. Box 2724, 100080 Beijing, China and Department of Materials Engineering, Dalian University of Sciences and Technology, 116024 Dalian, China

K. H. Kuo
Beijing Laboratory of Electron Microscopy, Chinese Academy of Sciences, P.O. Box 2724, 100080 Beijing, China
(Received 19 January 1990; revised manuscript received 15 June 1990)

The two-dimensional decagonal quasicrystal has been found in many Al-M (M=transitional metal) alloys, very often coexisting with a large-unit-cell phase of similar composition and local structure. By introducing phasons in two orthogonal directions in the quasiperiodic plane perpendicular to the periodic tenfold axis, i.e., approximating the irrational golden mean τ with rational ratios of two consecutive Fibonacci numbers F_{n+1}/F_n, the Penrose pattern in this plane gradually becomes periodic with fairly large unit-cell parameters (1–3 nm). Some giant Al-M crystals with cubic, orthorhombic, and monoclinic symmetries have thus been derived as Penrose-tiling approximants of the decagonal quasicrystal, and their simulated electron diffraction patterns agreed fairly well with experiments.

I. INTRODUCTION

In a previous paper[1] we have studied the transformation of the two-dimensional (2D) decagonal quasicrystal (QC) to various one-dimensional (1D) QC's (Ref. 2) with periodicities following the Fibonacci series (13:8:5:3). The decagonal QC is *periodic* in the tenfold direction and *aperiodic* in the plane perpendicular to it.[3,4] In fact, this plane is nothing else but the Penrose pattern with two kinds of rhombus tiles arranged aperiodically along the ten or five twofold directions according to an infinite Fibonacci series: $F_0=0, F_1=1, \ldots, F_{n+1}=F_n+F_{n-1}$, with $F_{n+1}/F_n \to \tau$ when $n \to \infty$, where the golden mean $\tau=(1+\sqrt{5})/2$. If a phason or a tiling mistake is introduced in one of these twofold directions (the P direction after Fund *et al.*[4]), the Fibonacci series will terminate at a certain point, say F_n, and then this Fibonacci series will start anew until a second tiling mistake occurs again at F_n. Such a repetition will produce a periodic sequence of Fibonacci blocks. This corresponds in fact to the substitution of irrational τ by a rational F_{n+1}/F_n and therefore is called a Fibonacci approximant.[5] The higher the density of tiling mistakes (or phasons), the shorter the periodicity of this Fibonacci approximant.[1]

If phasons are also introduced in the second set of twofold directions of the decagonal QC (the D direction after Fung *et al.*[4]), then a three-dimensional (3D) periodic crystal will result. Following Entin-Wohlman, Klein, and Pavlovitch,[5] this is called a Penrose-tiling approximant of the decagonal QC in the present paper. We shall apply such an analysis to the occurrence of the giant Al-M crystals (lattice parameters in general greater than 1 nm) studied in this laboratory, such as the orthorhombic Al_3Pd (Ref. 6) and AlMnCu (Ref. 7), cubic $Al_{13}Cr_4Si_4$ (Ref. 8), hexagonal AlCrNi and AlMnNi (Ref. 9), and monoclinic $Al_{13}Fe_4$ (Refs. 4 and 10).

Earlier Entin-Wohlman, Kleman, and Pavlovitch,[5] Ishihara,[11] and Mosseri, Oguey, and Duneau[12] have discussed in details the geometry of the Penrose-tiling approximants, such as the size of the unit cell and its relation to some characteristic lattice vectors of the Penrose tiling, but they did not relate this to any crystal coexisting with the decagonal QC in rapidly solidified alloys. Ishii[13] recently has described all possible symmetry breakings from the icosahedral point group by the action of phason strains with the help of group theory and discussed, as Elser and Henley[14] and Henley[15] did earlier, the structures of the cubic α-(AlMnSi), hexagonal AlFeSi, orthogonal θ'-(Al_7Cr), and monoclinic $Al_{13}Fe_4$ as structural modulations or approximants induced by phasons in the *icosahedral* QC. Knowles[16] and Dmitrienko[17] have also discussed the cubic approximants with large unit cells in the Al-Li-Cu and Al-Mn *icosahedral* QC, respectively. However, our derivation of the various giant Al-M crystals is based on the Penrose-tiling approximants of the decagonal QC and is more simple and straightforward. Moreover, the giant Al-M crystals mentioned in the previous paragraph are found experimentally coexisting with the decagonal QC with a definite orientation relationship between them, and their electron diffraction patterns (EDP's), especially the strong diffraction spots, resemble the corresponding ones of the decagonal rather than those of the icosahedral QC. Furthermore, the effect of phasons is discussed in the present paper mainly in the reciprocal space, because it is straightforward to compare the EDP's of the decagonal QC with its various approximants.

In this paper we use the cut-and-project method from the high-dimensional space developed independently by Kalugin, Kitaev, and Levitov,[18] Duneau and Katz,[19] and Elser[20] to describe the Penrose tiling (i.e., the decagonal quasicrystal). Contrary to the model for the incommens-

urate structure, the model of Penrose tiling leads to the discontinuous phason. However, is there any possible means to obtain continous phasons for Penrose tiling? According to Kalugin and Levitov[21] and Levitov,[22] the symmetry group of the Penrose tiling belongs to the noncrystallographic group in the two-dimensional space and does not satisfy the nontransversality condition. Therefore, continous phasons cannot exist in it. However, the icosahedral quasicrystal satisfies the nontransversality condition and can have continuous phason strains. The phason shift discussed here occurs discontinuously by local flip of two different kinds of tiles of the Penrose tiling.[23]

II. PENROSE-TILING APPROXIMANTS

Figure 1 is the tenforld EDP of the decagonal QC in which the two sets of twofold directions, P's and D's are orthogonal to each other. Obviously, the electron diffraction spots are distributed aperiodically in either the P's or the D's directions, both at 36° apart. From Fig. 1 it seems that the ten P_2 spots are stronger than D_2 spots, but in reality the D_2 spots are stronger than P_2 spots in the tenfold EDP of the decagonal QC. The calculated EDP (Fig. 1) is the Fourier transform of the 2D quasilattice without decoration, whereas the experimental EDP is that of the real structure. If the electron diffraction spots, under the action of the linear phason strain, become gradually periodic in one P and one D direction at 90° with each other, the decagonal QC will transform into an orthorhombic crystal. On the other hand, if the electron diffraction spots in two P or two D directions at 36° or 72° apart become periodic, then a rhombus discussed earlier by Entin-Wohlman, Kleman, and Pavlovitch[5] will result. This is in fact a base-centered orthorhombic crystal; see Fig. 2.

According to the linear phason theory of QC (Refs. 24 and 25) as briefly outlined in our previous paper,[1] the diffraction spot $G^{\parallel}$ will occur at the end of the reciprocal vector $\mathbf{G}^{\parallel'}$ by the action of phason strain $\mathbf{M}$,

$$\mathbf{G}^{\parallel'}=\mathbf{G}^{\parallel}+\mathsf{M}\cdot\mathbf{G}^{\perp}\ , \tag{1}$$

where M is a second-rank tensor

$$\mathsf{M}=\begin{bmatrix} m_{11} & m_{12} \\ m_{21} & m_{22} \end{bmatrix} \tag{2}$$

and $\mathbf{G}^{\parallel}$ and $\mathbf{G}^{\perp}$ are the reciprocal vectors in the physical and complementary (or perpendicular) spaces, respectively,

$$\mathbf{G}^{\parallel}=\frac{\sqrt{2}\mathbf{a}^*}{\sqrt{5}}\sum_{i=1}^{5} n_i\mathbf{e}_i^{\parallel}\ ,$$

$$\mathbf{e}_i^{\parallel}=(\cos(2j\pi/5),\sin(2j\pi/5)),\quad j=i-1\ , \tag{3}$$

$$\mathbf{G}^{\perp}=\frac{\sqrt{2}\mathbf{a}^*}{\sqrt{5}}\sum_{i=1}^{5} n_i\mathbf{e}_i^{\perp}\ ,$$

$$\mathbf{e}_i^{\perp}=(\cos(4j\pi/5),\sin(4j\pi/5)),\quad j=i-1\ . \tag{4}$$

In the case of 2D to 1D QC transformation,[1] $m_{12}=m_{21}=m_{22}=0$ (or $b=c=d=0$ in Ref. 1). With the increase of the absolute value of m_{11} (a in Ref. 1), the quasiperiodic distribution of electron diffraction spots along the P direction of the decagonal QC (see Fig. 1) becomes gradually periodic and its periodicity decreases accordingly. For instance, as m_{11} changes from -0.02, 0.055, -0.145 to 0.38, the number of equally spaced diffraction spots between the central one to spot P_2 is 13, 8, 5, and 3, respectively. These m_{11} values were found then by trial and error,[1] but now they can be calculated according to a simple geometrical analysis. As shown in Table I, they correspond to $-1/\tau^8$, $1/\tau^6$, $-1/\tau^4$, and $1/\tau^2$ obtained by substituting $\frac{13}{8}$, $\frac{8}{5}$, $\frac{5}{3}$, and $\frac{3}{2}$, respectively, for τ. It is interesting to note that the periodicity is almost proportional to F_{n+1}.

By a transformation of the coordinated system, formula (2) can be converted to

$$\mathsf{M}=\begin{bmatrix} m_{11} & 0 \\ 0 & m_{22} \end{bmatrix} \tag{2'}$$

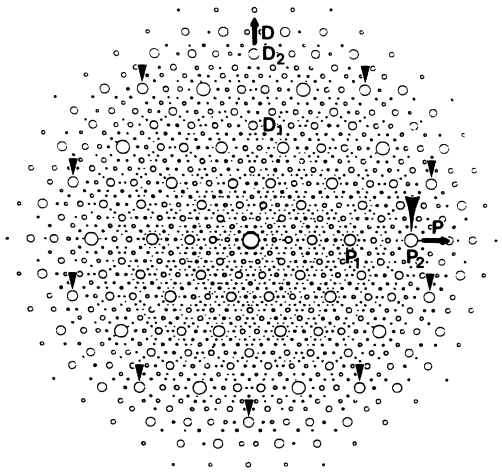

FIG. 1. Simulated tenfold electron diffraction pattern of the 2D decagonal quasicrystal. P and D indicate the two sets of twofold directions orthogonal to each other.

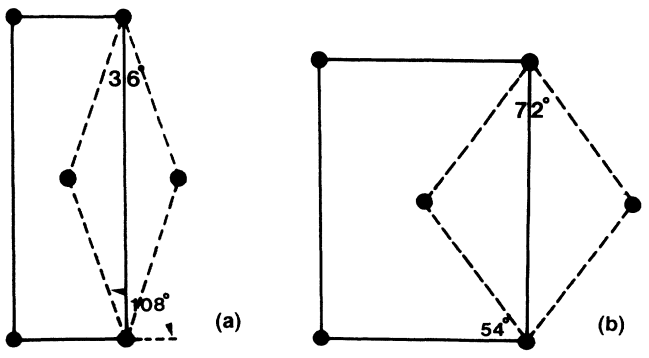

FIG. 2. (a) Monoclinic unit cell of $Al_{13}Fe_4$ ($\beta=72°$) and (b) the (110) projection of a face-centered-cubic unit cell of $Al_{13}Cr_4Si_4$ can be described approximately as base-centered orthorhombic cells. They can also be visualized as 2D thin (36°) and thick (72°) Penrose rhombi.

TABLE I. Phason strain tensors m_{11}, m_{22} and lattice parameters of some Penrose-tiling approximants (a_R=0.40 nm).

n	F_{n+1}/F_n	m_{11}	a_P (nm)	m_{22}	a_D (nm)
2	2/1	-1	0.89	$1/\tau$	0.76
3	3/2	$1/\tau^2$	1.45	$-1/\tau^3$	1.23
4	5/3	$-1/\tau^4$	2.34	$1/\tau^5$	1.99
5	8/5	$1/\tau^6$	3.79	$-1/\tau^7$	3.23
6	13/8	$-1/\tau^8$	6.13	$1/\tau^9$	5.22
⋮	⋮	⋮	⋮	⋮	⋮

with the new coordinated axes lying along the main axes of the second-rank tensor and in this case m_{11} and m_{22} are independent. In the following we discuss the transformation of the decagonal quasicrystal by the action of phasons to a related orthorhombic crystalline phase belonging to one of the subgroups of the decagonal group $10/mmm$. The crystalline phase will inherit the orthorhombic symmetry of the decagonal quasicrystal (i.e., two perpendicular twofold axes P and D in Fig. 1). From (1) and (2′), the x coordinate of $G^{\parallel}$ along the P direction will depend only on m_{11} and y along the D direction only on m_{22}. Thus, we can treat the phason strain independently along these two perpendicular directions.

From Fig. 1 it is obvious that $G_{P2}/G_{P1}=\tau$. After introducing linear phason strain, it can be approximated by the rational ratio F_{n+1}/F_n. Since the indices of these two spots are $10\bar{2}\,\bar{2}0$ and $10\bar{1}\,\bar{1}0$ (see Ref. 19), respectively, one obtains from Eqs. (3) and (4)

$$G^{\parallel'}(P_2)=(\sqrt{2}a^*/\sqrt{5})[1+2\tau+m_{11}(3-2\tau)] ,$$

$$G^{\parallel'}(P_1)=(\sqrt{2}a^*/\sqrt{5})[1+\tau+m_{11}(2-\tau)] ,$$

where a^* is the reciprocal-lattice constant in 5D space. Equating the ratio of $G^{\parallel'}(P_2)/G^{\parallel'}(P_1)$ to F_{n+1}/F_n and after some manipulation, we find (for a detailed derivation, see the Appendix)

$$m_{11}=(\tau F_{n-2}-F_{n-1})/(F_{n-3}+\tau F_{n-2}) =(-1)^{n+1}\tau^{-2(n-2)} . \quad (5)$$

In the 1D case,[1] substituting F_{n+1}/F_n for τ will yield F_{n+1} equally spaced spots between the transmitted beam and spot p_2, therefore $a_P=F_{n+1}/G^{\parallel'}(P_2)$. But in the 2D case, a factor of 2 has to be added into this relationship. Looking at the base-centered orthorhombic unit cell in Fig. 2(a), the reciprocal unit cell will also be a base-centered one. In other words, if there are F_{n+1} spots appearing up to spot P_2, an equal number of spots will be extinct due to base centering. Therefore, there will be altogether $2F_{n+1}$ spots along the P or D direction in the 2D case. This can be proved rigorously either in the real or reciprocal space, but it is too lengthy to be given here. Thus (see also the Appendix),

$$a_P=2F_{n+1}/G^{\parallel'}(P_2)=\sqrt{5}a_R\tau^{n-2} , \quad (6)$$

where a_R is the edge length of the Penrose rhombus. Thus it is clear that $|m_{11}|$ varies with n in a $1/\tau^2$ relationship and a_P with a τ relationship, as shown in Table I. Between two successive F_n's the phason strain reverses its direction, therefore m_{11} also changes its sign.

If the phason is also introduced in the D direction in Fig. 1, the electron diffraction spots in this direction also become periodic. Now the indices of spots D_2 and D_1 are, respectively, $021\bar{1}\,\bar{2}$ and 10022, and similarly we obtain

$$m_{22}=(\tau F_{n-1}-F_n)/(F_{n-3}+\tau F_{n-2}) =(-1)^n\tau^{-2(n-2)/\tau} \quad (7)$$

and

$$a_D=\sqrt{5}a_R\tau^{n-1}/[(1+\tau^2)]^{1/2} . \quad (8)$$

Obviously, $|m_{22}|$ also varies with n or F_{n+1}/F_n in a $1/\tau^2$ relation and a_D in a τ relation as their counterparts in the P direction. Moreover, for the same n or F_{n+1}/F_n ratio, $m_{22}/m_{11}=-1/\tau$ and $a_P/a_D=2\sin 36°=[(1+\tau^2)]^{1/2}/\tau$.

Combinations of these a_P and a_D in two orthogonal directions will give a series of orthorhombic Penrose-tiling approximants. For certain special cases, centered orthorhombic unit cells can be approximated as face centered cubic or monoclinic unit cells. As discussed in connection with Fig. 2, these are equivalent to substituting F_{n+1}/F_n for τ along two P or two D directions at 72° and 36°, respectively. These will be illustrated in the following.

III. GIANT Al-M CRYSTALS

Many binary and ternary Al-rich Al-M intermetallic compounds with large unit cells were known and the crystal structure of a number of them has been solved. They have many common characteristic features. The most striking feature among these crystal structures is the icosahedral cluster with the smaller M atom located at its center and the larger Al atoms at its vertices. These icosahedral clusters, somewhat deformed to conform to the symmetry of the crystal lattice, form complicated skeletons in three dimensions. Their x-ray diffraction pattern showed characteristic fivefold[26] and tenfold[27] rotational symmetries which were noted already in the beginning of the 1950s. Another feature is the large lattice parameters, generally 1–3 nm, which are not common in intermetallic compounds. In Table II we have listed a few of them which have been studied before in this laboratory in connection with the decagonal QC and now as examples of its Penrose-tiling approximants. It is to be

TABLE II. Giant Al-*M* crystals coexisting with the decagonal quasicrystal (the lattice parameter in bold is that parallel to the tenfold axis and those in parentheses are the a_P and a_D of the Penrose approximants in Table I).

Symmetry	Crystal	Reference No.[a]	Lattice parameters (nm) a	b	c
Cubic	$Al_{13}Cr_4Si_4$	8	1.092 (1.23)		
Orthorhombic	$Al_{11}Mn_4$	30	**1.479** (1.45)	**1.242**	1.259 (1.23)
	AlMnCu	7	1.48 (1.45)	1.26 (1.23)	**1.24**
	"Al_3Pd"	6	2.34 (2.34)	**1.67**	1.23 (1.23)
	AlMnNi,*C3I*	31	**1.24**	2.40 (2.34)	3.27 (3.22)
Monoclinic[b]	$Al_{13}Fe_4$	10	0.7745 (0.76)	**0.8083**	2.377 (2.34)

[a]The references given here deal with the crystalline phase coexisting with the decagonal QC and their structural relationship. Original references concerning the crystal data of these Al-*M* compounds can be found there.

[b]The lattice parameters given here for $Al_{13}Fe_4$ are those of a centered orthorhombic unit cell calculated, with slight deformation, from the monoclinic cell with $a=1.5489$, $b=0.8083$, $c=1.2476$ nm, and $\beta=107.71°$.

noted that all these Al-*M* compounds, except the cubic $Al_{13}Cr_4Si_4$, have a lattice parameter roughly equal to 0.81, 1.23, or 1.64 nm, which are known to be the periodicity along the tenfold axis of the 2D decagonal QC.[28] In the case of this cubic crystal, it was found that the [110] direction is parallel to this axis[8] and if $a=1.15$ nm, $d_{110}=0.82$ nm. What we need to do now is to find the 2D Penrose-tiling approximants perpendicular to this direction.

A. Orthorhombic crystals

Figure 3(b) shows the [010] EDP of the metastable "Al_3Pd" and its strong diffraction spots forming concentric decagons are quite similar to those of the tenfold EDP of the coexisting 2D decagonal QC.[6] Its b parameter is 1.62 nm, the same as the periodicity of the Al-Pd decagonal QC and its a and c parameters are 2.34 and 1.23, nm, respectively. Using these values and the

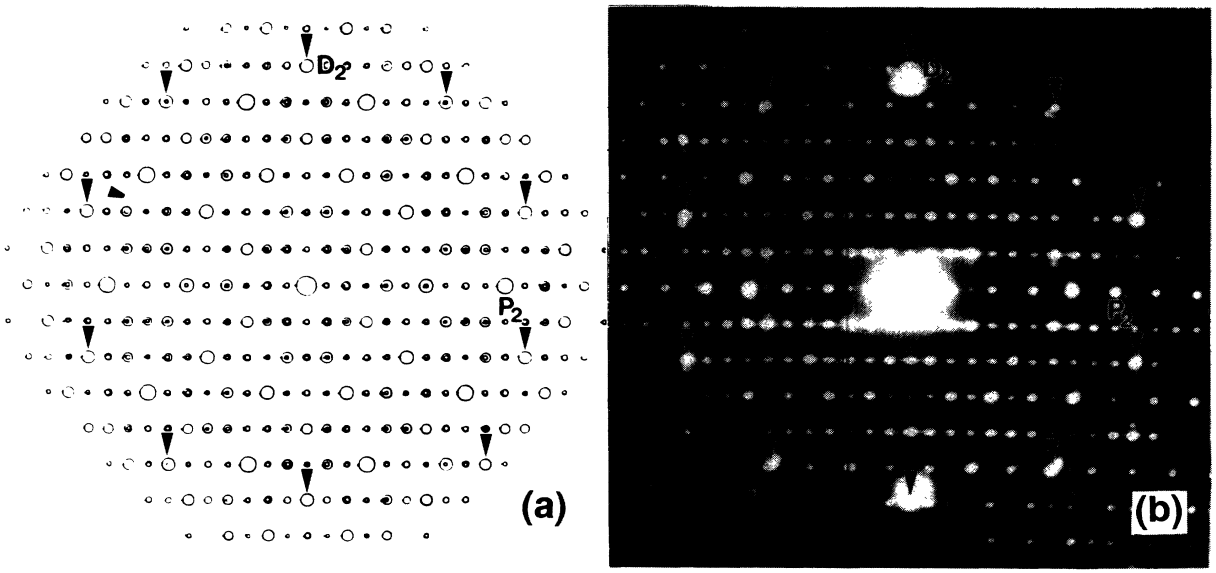

FIG. 3. (a) Simulated and (b) experimental (Ref. 6) [010] electron diffraction patterns of the orthorhombic "Al_3Pd."

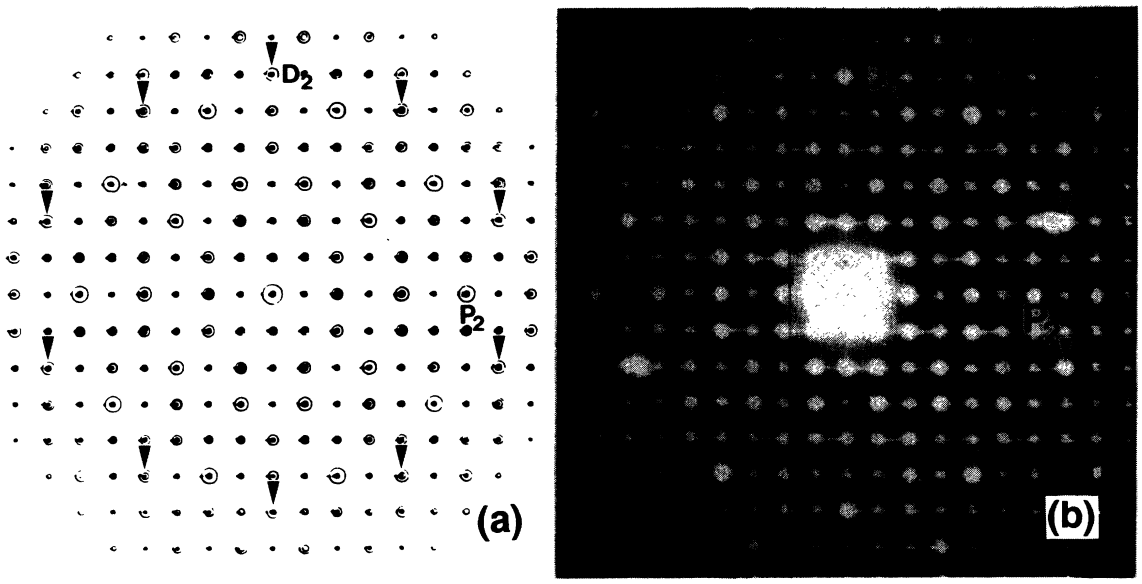

FIG. 4. (a) Simulated and (b) experimental (Ref. 7) [001] electron diffraction patterns of orthorhombic $Al_{65}Mn_{20}Cu_{15}$ isostructural with $Al_{11}Mn_4$.

F_{n+1}/F_n ratios given in Table II, the calibrated edge length of the 2D Penrose rhombi a_R is 0.40 nm, similar to the value 0.39 nm given earlier in the Al-Mn decagonal QC.[29] The phason strain tensor is now $M=(1/\tau^4)[-1,0/0,-\tau]$ and the simulated EDP is shown in Fig. 3(a) which matches well the experimental EDP in Fig. 3(b). Comparing with Fig. 1, the ten strong spots marked with arrowheads in Fig. 3(a) can still be seen but there are less spots because several spots in Fig. 1, under the influence of the linear phason strain M, have moved to the same spot in Fig. 3(a), as shown by the concentric circles in it.

The orthorhombic phase found in a rapidly solidified $Al_{65}Mn_{20}Cu_{15}$ alloy[7] is isostructural with $Al_{11}Mn_4$ (space group *Pnma*) and both were found to occur together with the decagonal QC. Moreover, one of their lattice parameters is about 1.24 nm and this axis is found to be parallel to the tenfold axis of the decagonal QC. The a and b parameters for the $Al_{65}Mn_{20}Cu_{15}$ phase are 1.48 and 1.26 nm, respectively, which compare favorably with the a_P and a_D of 1.45 and 1.23 nm, respectively, in Table I. Now the F_{n+1}/F_n for the P and D directions is the same and $M=(1/\tau^3)[\tau,0/0,-1]$. Again the simulated EDP matches well the experimental one, as shown in Fig. 4.

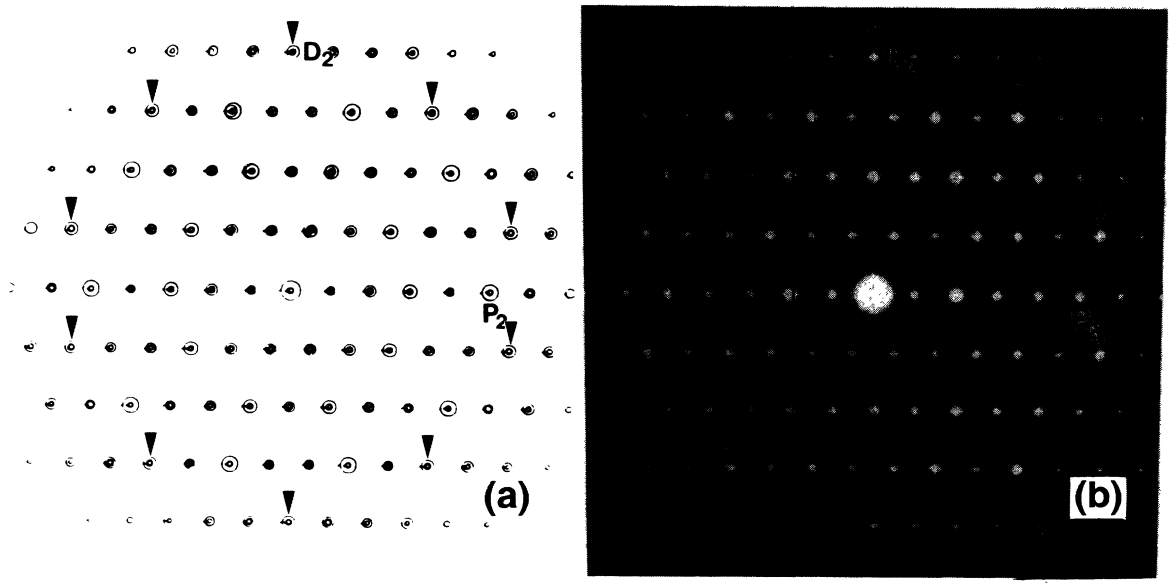

FIG. 5. (a) Simulated and (b) experimental (Refs. 4 and 10) [010] electron diffraction patterns of monoclinic $Al_{13}Fe_4$.

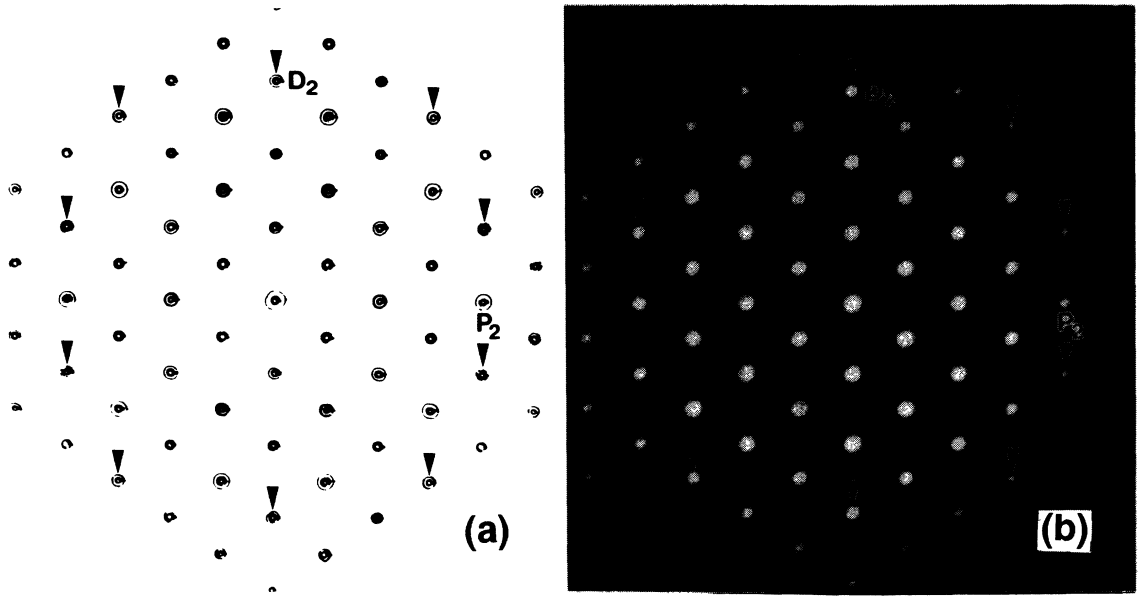

FIG. 6. (a) Simulated and (b) experimental (Ref. 8) [010] electron diffraction pattern of face-centered-cubic $Al_{13}Cr_4Si_4$.

The agreement between the calculated and experimental lattice parameters is fairly good too for $Al_{11}Mn_4$ (see Table II).

Another orthorhombic crystal of interest is $Al_{60}Mn_{11}Ni_4$ ($C3I$) (Ref. 30) whose lattice parameters also agree with the Penrose-tiling approximant as shown in Table II. This giant crystal gives EDP's of various orientations quite similar to those of the decagonal QC coexisting with it.[31] However, this Penrose-tiling approximant is base-centered orthorhombic whereas the crystalline phase actually found is simple orthorhombic, though its structure is still unknown. The disappearance of centering can either be due to a slight deformation or to a change in the distribution of atoms during the QC—crystal transformation.

B. Cubic $Al_{13}Cr_4Si_4$ and monoclinic $Al_{13}Fe_4$

As mentioned above, under certain conditions we can even get cubic and monoclinic crystals as Penrose-tiling approximants of the decagonal QC, see Table II. For the monoclinic $Al_{13}Fe_4$, its $\beta=107.71°$ is very close to the 108° belonging to the tenfold symmetry of the decagonal QC. This can be treated either as a 36° rhombus or as a centered rectangular lattice with an axial ratio of tan72°, as shown in Fig. 2(a). In Table I, the ratio of $2.34/0.76=2\tau^2\sin36°=\tan72°$, and the lattice parameter ratio of the centered rectangular cell calculated from those of the monoclinic cell, 2.377/0.7745, is fairly close to it. Figure 5 shows the simulated and experimental[4,10] EDP's.

In the case of a 72° rhombus, the unit cell can be visualized as a centered rectangular cell close to that of the (110) of a face-centered-cubic cell [the corresponding angle is 54.7° compared with 54° shown in Fig. 2(b)]. The axial ratio in Fig. 2(b) is equal to tan36°, roughly the same as the ratio of $0.894/1.23\approx2\sin36°/\tau$. Our calculated parameter $a=1.23$ nm is about 10% larger than the experimental 1.09 nm, but this is obtained from an $a_R=0.40$ nm of Al_3Pd. With some modification of this value, a better agreement can be arrived. Figure 6 gives the simulated and experimental[8] [110] EDP's.

Entin-Wohlman, Kleman, and Pavlovitch[5] have dis-

TABLE III. Some Al-M compounds with giant unit cells.

Compounds	Reference No.	Space group	Lattice parameters (nm) a	b	c
$Al_{60}Mn_{11}Ni_4$	32	*Bbmm*	2.38	1.25	0.755
$Al_{20}Mn_3Cu_2$	27		2.42	1.25	0.772
AlMnZn($T3$)	33	*Bbmm*[a]	2.38	1.26	0.778
$Al_{24}Mn_5Zn$	27		2.51	2.48	3.03
Al_7Cr	34		2.48	2.47	3.02

[a]Originally reported as *Cmcm* with $a=0.778$, $b=2.38$, $c=1.26$ nm (Ref. 33).

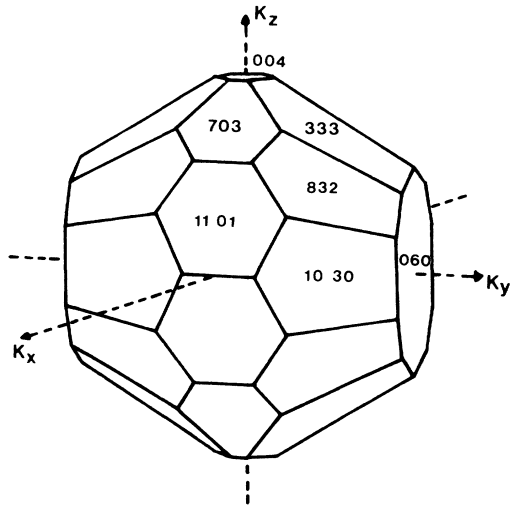

FIG. 7. The first Brillouin zone of $Al_{60}Mn_{11}Ni_4$ showing almost tenfold rotational symmetry around the [010] direction [Robinson (Ref. 27)].

cussed earlier the Penrose-tiling approximants from the 36° and 72° rhombi by introducing periodically phasons to their deflated patterns. Our centered rectangular cell treatment is in principle equivalent to their rhombic approximants.

IV. DISCUSSION

Evidently, the above derivation of various crystal lattices from the 2D quasilattice is a rather naive one, since it has neither touched the arrangement of Penrose tiles nor the atomic decoration of them. Nevertheless, it accounts fairly well for the lattice relationship between these large unit cell Al-M compounds and the 2D decagonal QC as well as for the ten strong spots forming decagons in their EDP's. In addition to these giant Al-M compounds coexisting with the 2D decagonal QC, there are still some others which have not yet been found together with this QC, such as those studied mainly by Robinson[27,32] (see Table III).

It is to be noted that the first group of Al-Mn-M compounds have a and c parameters quite close to the 2.34 and 0.76 nm given in Table I or those of $Al_{13}Fe_4$ in Table II. Their b parameter of 1.25–1.26 nm agrees well with the periodicity of 1.24 nm of the Al-Mn decagonal QC. Furthermore, their $h0l$ reflections are strong and show a tenfold distribution from which Robinson[27] drew the first Brillouin zone displaying an approximate tenfold symmetry along the k_y axis, as shown in Fig. 7. In other words, these Al-M compounds can very well be described by the same scheme as those presented in Table II. Their composition can be written as $Al_4(Mn,M)$, the same as the Al_4Mn decagonal QC. All these facts point to the possibility of finding these compounds together with the decagonal QC in rapidly solidified alloys.

The second group of giant orthorhombic Al-M compounds listed in Table III are also of interest simply because their lattice parameters are almost the double of those of $Al_{11}Mn_4$ or the $Al_{65}Mn_{15}Cu_{20}$ compound discussed in Sec. III. This can possibly occur if there is some ordering in these ternary compounds so that their parameters have to be doubled. As a matter of fact, Robinson[27] has already noticed that all reflections with h and k odd are very weak indeed. It would be of interest to see whether these compounds will occur together with the decagonal QC or not in rapidly solidified alloys.

This lattice correspondence between the decagonal QC and the relevant gian Al-M crystals is of course valuable for the study of the formation of this group of large unit-cell Al-M crystals as well as the occurrence of the decagonal QC in the Al-M alloys. A detailed study of the tiling or even better the atomic decoration of the tiles in these two categories of structures will greatly advance our knowledge of them. This will be further pursued in this laboratory.

ACKNOWLEDGMENTS

The authors thank D. Yashusi Ishii of the Institute of Solid State Physics, University of Tokyo, for many inspiring discussions and the improvements of the first draft of this paper. This project was supported partly by the National Natural Science Foundation of China.

APPENDIX

The Fibonacci series can be written as $F_{n+1}=F_n+F_{n-1}$, $F_0=0$, $F_1=1$. Since $\tau^2=1+\tau$, we have

$$\begin{aligned}\tau F_{n+1}+F_n &=(1+\tau)F_n+\tau F_{n-1}\\ &=\tau(\tau F_n+F_{n-1})\\ &=\tau^n(\tau F_1+F_0)\\ &=\tau^{n+1}.\end{aligned}$$

Similarly,

$$F_{n+1}-\tau F_n=(-\tau)^{-n}$$

and

$$(\tau^2+1)F_n=\tau^{n+1}+(-\tau)^{-(n-1)}.$$

These relationships will be used in deriving Eqs. (5) and (6) as follows. For Eq. (5),

$$\begin{aligned}m_{11}&=(\tau F_{n-2}-F_{n-1})/(F_{n-3}+\tau F_{n-2})\\ &=-(-\tau)^{-(n-2)}/\tau^{(n-2)}\\ &=(-1)^{n+1}\tau^{-2(n-2)},\end{aligned}$$

and for Eq. (6),

$$
\begin{aligned}
a_P &= 2F_{n+1}/G^{\parallel'}(P_2) = 2\sqrt{5}F_{n+1}/\{\sqrt{2}a^*[1+2\tau+m_{11}(3-2\tau)]\} \\
&= \sqrt{2}\sqrt{5}aF_{n+1}/[\tau^3+m_{11}(-\tau^{-3})] \\
&= 5a_R F_{n+1}/[\tau^3+(-1)^{n_\tau-2n+1}] \\
&= 5a_R\tau^{n-1}F_{n+1}/[\tau^{n+1+1}+(-1)^{n+1-1}\tau^{-(n+1-1)}] \\
&= 5a_R\tau^{n-1}F_{n+1}/[(\tau^2+1)F_{n+1}] = \sqrt{5}a_R(\tau+1/\tau)\tau^{n-1}/(\tau^2+1) = \sqrt{5}a_R\tau^{n-2} .
\end{aligned}
$$

Equations (7) and (8) can be derived accordingly.

[1]H. Zhang and K. H. Kuo, Phys. Rev. B **41**, 3482 (1990).
[2]L. X. He, X. Z. Li, Z. Zhang, and K. H. Kuo, Phys. Rev. Lett. **61**, 1116 (1988).
[3]L. Bendersky, Phys. Rev. Lett. **55**, 1461 (1985).
[4]K. K. Fung, C. Y. Yang, Y. Q. Zhou, J. G. Zhou, W. S. Zhan, and B. G. Shen, Phys. Rev. Lett. **56**, 2060 (1986).
[5]G. Entin-Wohlman, M. Kleman, and A. Pavlovitch, J. Phys. (Paris) **49**, 587 (1988).
[6]L. Ma, R. Wang, and K. H. Kuo, Scr. Metall. **22**, 1791 (1988).
[7]L. X. He and K. H. Kuo (private communication).
[8]H. Zhang, D. H. Wang, and K. H. Kuo, J. Mater. Sci. **24**, 2981 (1989).
[9]W. L. Zhou, X. Z. Li, and K. H. Kuo, Scr. Metall. **23**, 1571 (1989).
[10]X. D. Zou, K. K. Fung, and K. H. Kuo, Phys. Rev. B **35**, 4526 (1987).
[11]K. N. Ishihara, Mater. Sci. Forum **22-24**, 223 (1987).
[12]R. Mosseri, C. Oguey, and M. Duneau, in *Quasicrystalline Materials,* edited by Ch. Janot and J. M. Dubois (World Scientific, Singapore, 1988), p. 224.
[13]Y. Ishii, Phys. Rev. B **39**, 11862 (1989); (unpublished).
[14]V. Elser and C. Henley, Phys. Rev. Lett. **55**, 2883 (1985).
[15]C. Henley, J. Non-Cryst. Solids, **75**, 91 (1985).
[16]K. W. Knowles, in *Quasicrystalline Materials,* edited by Ch. Janot and J. M. Dubois (World Scientific, Singapore, 1988), p. 158.
[17]V. E. Dmitrienko, Pis'ma Zh. Eksp. Teor. Fiz. **45**, 31 (1987) [JETP Lett. **45**, 38 (1987)].
[18]P. A. Kalugin, A. Yu. Kitaev, and L. S. Levitov, Pis'ma Zh. Eksp. Teor. Fiz. **41**, 119 (1985) [JETP Lett. **41**, 145 (1985)]; J. Phys. Lett. **46**, 601 (1985).
[19]M. Duneau and A. Katz, Phys. Rev. Lett. **54**, 1730 (1985).
[20]V. Elser, Acta. Crystallogr. Sec. A **42**, 36 (1985).
[21]P. A. Kalugin and L. S. Levitov, Int. J. Mod. Phys. B **3**, 887 (1989).
[22]L. S. Levitov, J. Phys. (Paris) **50**, 3181 (1989).
[23]P. Bak, Scr. Metall. **20**, 1199 (1986).
[24]T. C. Lubensky, J. E. S. Socolor, P. J. Steinhardt, P. A. Bancel, and P. A. Heiney, Phys. Rev. Lett. **57**, 1440 (1986).
[25]P. M. Horn, W. Menzfeldt, D. P. DiVincenzo, J. Toner, and R. Gambino, Phys. Rev. Lett. **57**, 1444 (1986).
[26]K. Robinson and P. J. Black, Philos. Mag. **44**, 1392 (1953).
[27]K. Robinson, Philos. Mag. **43**, 775 (1952).
[28]X. Z. Li and K. H. Kuo, Philos. Mag. Lett. **58**, 167 (1988).
[29]W. Steurer and J. Mayer, Acta Crystallogr. Sec. B **45**, 355 (1989).
[30]J. D. Fitzgerald, R. L. Withers, A. M. Stewart, and A. Calka, Philos. Mag. B **58**, 15 (1988).
[31]G. Van Tendeloo, J. Van Landuyt, S. Amelinckx, and S. Ranganathan, J. Micros. **149**, 1 (1988).
[32]K. Robinson, Acta Crystallogr. **7**, 494 (1954).
[33]A. Damjanovic, Acta. Crystallogr. **14**, 982 (1961).
[34]K. Little, Dissertation, University of Oxford, 1949.

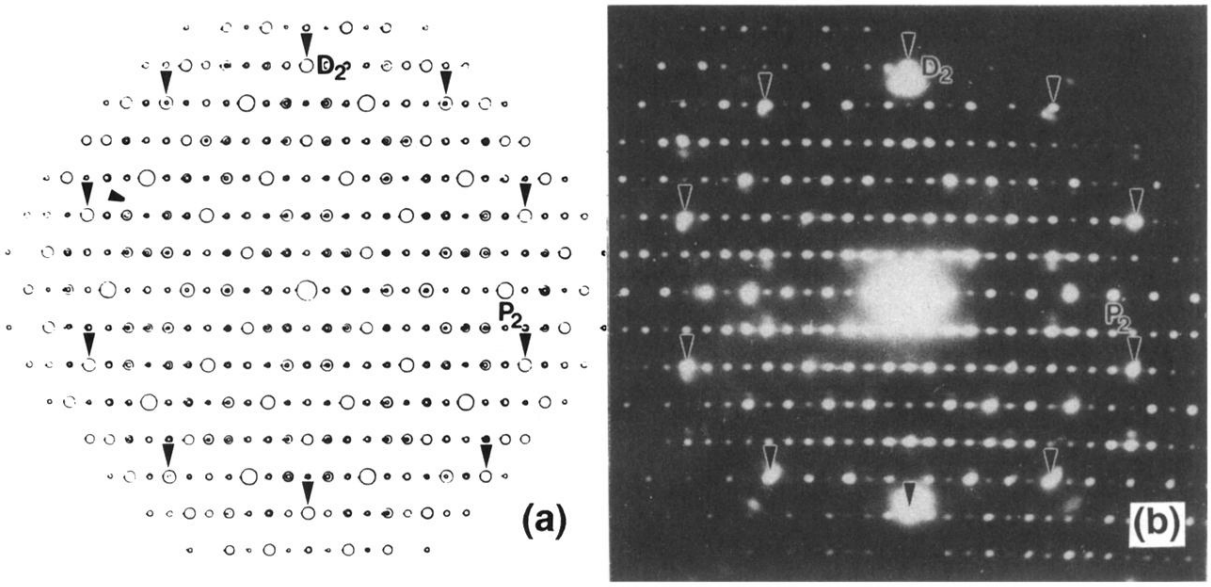

FIG. 3. (a) Simulated and (b) experimental (Ref. 6) [010] electron diffraction patterns of the orthorhombic "Al_3Pd."

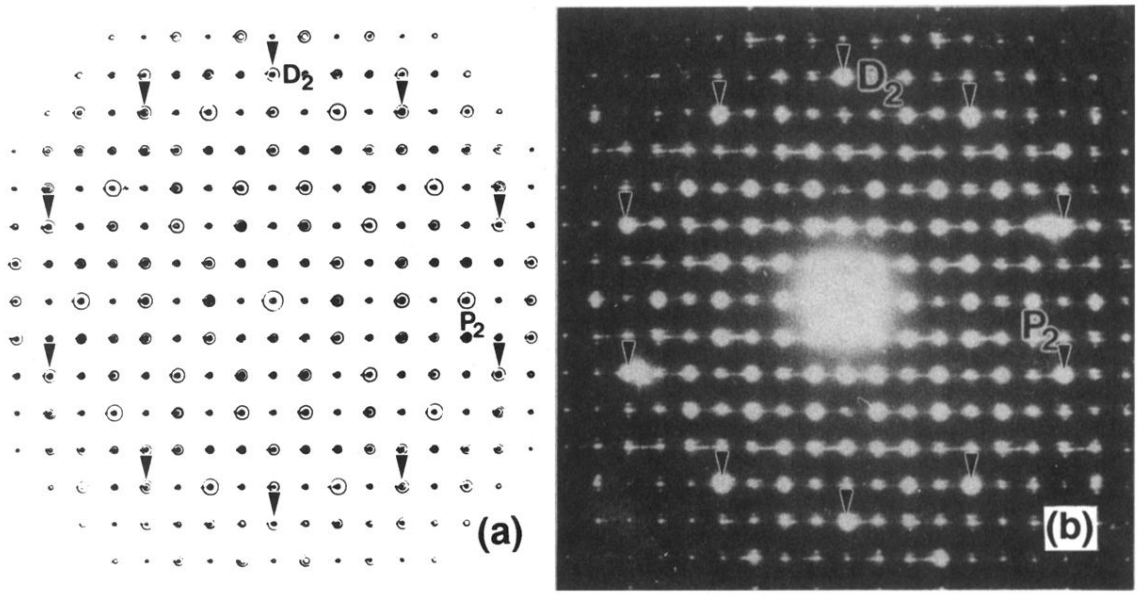

FIG. 4. (a) Simulated and (b) experimental (Ref. 7) [001] electron diffraction patterns of orthorhombic $Al_{65}Mn_{20}Cu_{15}$ isostructural with $Al_{11}Mn_4$.

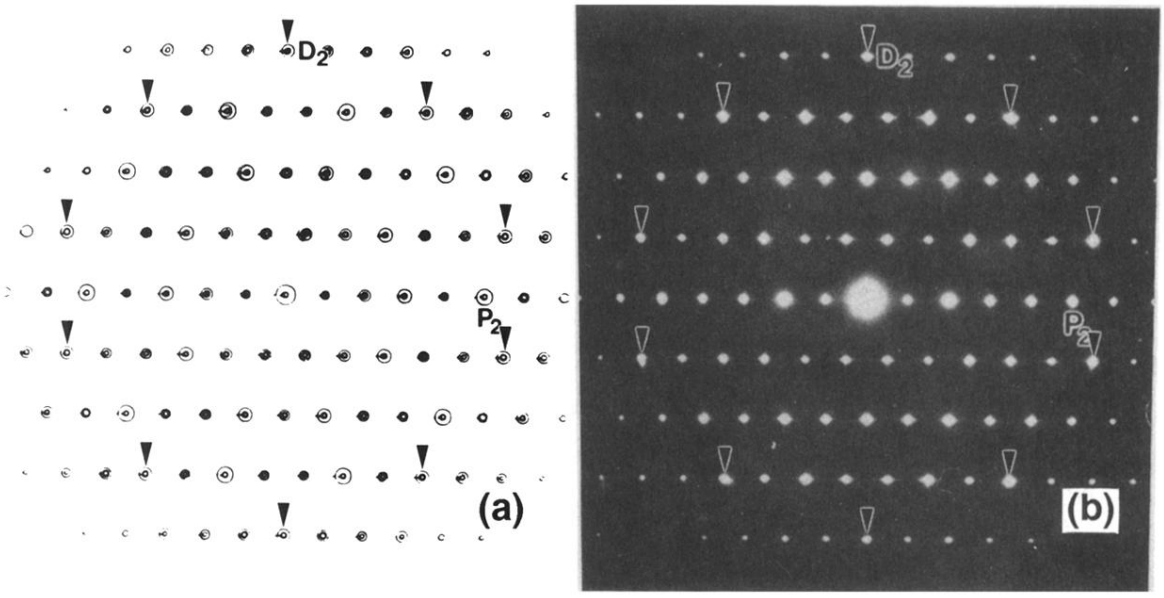

FIG. 5. (a) Simulated and (b) experimental (Refs. 4 and 10) [010] electron diffraction patterns of monoclinic $Al_{13}Fe_4$.

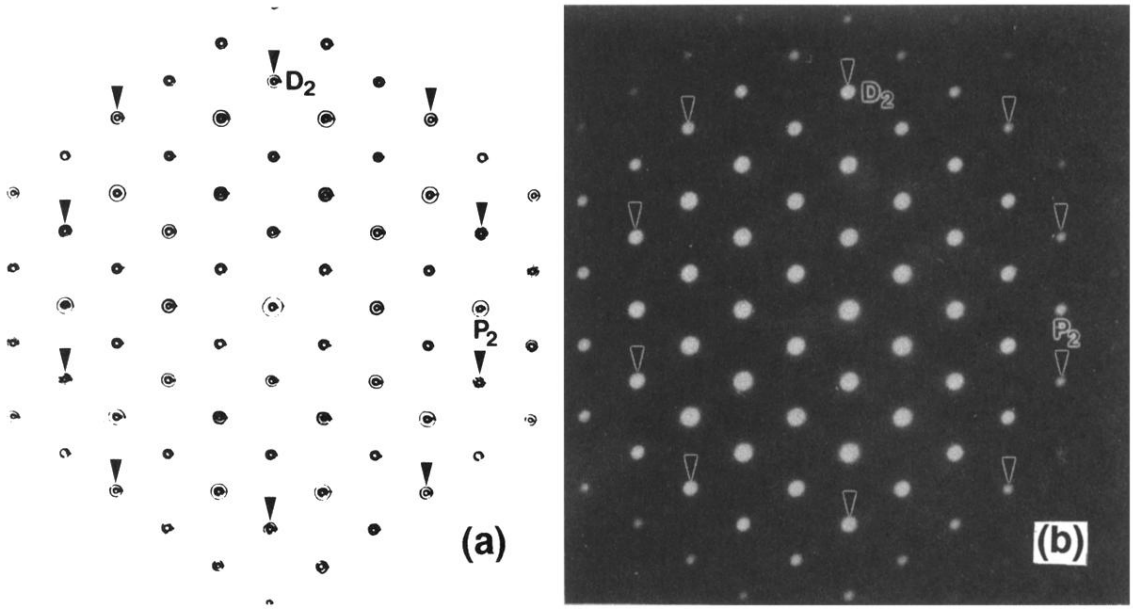

FIG. 6. (a) Simulated and (b) experimental (Ref. 8) [010] electron diffraction pattern of face-centered-cubic $Al_{13}Cr_4Si_4$.